

# Capacity improvement analysis of 3D-beamforming in small cell systems

Wenlong XU

*School of Information and Electronics, Beijing Institute of Technology, Beijing 100081, China*

Received 27 January 2017/Accepted 27 February 2017/Published online 25 August 2017

**Abstract** We analyze three dimensional (3D) beamforming characteristics and applications in wireless small cell communication based on physical structure of array antenna, addressing on the 3D beampattern property of planar rectangular array antenna beamforming. Firstly, array manifold vector is formulated based on rectangular array antenna, and formulas are derived pertaining to antenna beampattern parameters in detail. Secondly, the effect of array antenna configuration on 3D beamforming is analyzed. Thirdly, 3D beamforming is extended and applied to massive MIMO small cell wireless communication scenario by analyzing capacity gain of single small cell over that of two dimensional (2D) beamforming. Numerical results are presented to show properties of the 3D beamforming.

**Keywords** wireless communications, fifth generation (5G), massive MIMO, small cell, 3D beamforming

**Citation** Xu W L. Capacity improvement analysis of 3D-beamforming in small cell systems. *Sci China Inf Sci*, 2018, 61(2): 022305, doi: 10.1007/s11432-017-9084-8

## 1 Introduction

Recent researches have shown a potential trend of wireless communications that in the next ten years a factor of thousand increase of wireless network capacities is expected to be realized by massive multiple-input multiple-output (MIMO) network densification through adaptation of small cell technologies. To meet the demand for high system capacity, effort has been made continuously in the aspects of increasing the efficiency of existing resources and exploring new available resources suitable for wireless communications [1–5]. Investigations aiming to improve efficiency of present resources have attracted research interest for more than four decades, created abundant outcomes in both theory and application scenarios, such as, technology development from single-user (SU) system to multiple-user (MU) system; from single-input single-output (SISO) to MIMO and further, to massive MIMO; From single-mode to multiple-mode system (i.e., time domain to space-time domain processing architecture); from orthogonal to non-orthogonal coding, modulation and estimation system.

Performance bottleneck has been emerging in diverse aspects for further leveraging the performance of currently available resources (such as, time, frequency and code) in wireless communications. As a result, developing new available resources attracts worldwide research interest. Among them, research on beamforming technology is a hot topic [6, 7]. The rapid increasing challenges emerge between the scarce of available resources, such as time, frequency spectrum and code that can be employed in wireless communications, and the dramatically increasing demand for higher data rate, throughput and system capacity, make spatial resource more important than ever in wireless communication systems [8].

---

Email: xu@bit.edu.cn

Beamforming refers to the function of smart antennas which controls the properties of electromagnetic wave radiation pattern in an array antenna by aligning the amplitude and phase of transmit/receive signals in array antenna elements thus increasing array antenna gains in intended angle of directions, at the same time, compressing gains in uninterested angle of directions where interference signals exist, forming a desired beam pattern.

In general, beamforming techniques encompass two types, switched beams and adaptive beamforming systems. Switched beam systems [9] create fixed beam patterns. A decision has to be made as to which beam to choose at a given time based upon the demand of system. On the contrary, adaptive beamforming technique synthesizes beams in arbitrary directions of interest while simultaneously nulling interfering signals in unintended angles of direction.

Thus, with characteristics of directing narrow beams toward users of interest while nulling those users of uninterested, beamforming will increase signal-to-interference-plus-noise ratio (SINR) of intended users, providing multiple benefits for the system, such as, higher system capacities, lower transmit power, and greater frequency reuse factor within a given area than two dimensional (2D) scenario. For this reason, beamforming technique in wireless communications has been attracting increasing research interest in recent years, evolved from 2D to three dimensional (3D) beamforming.

While using the same principle as 2D beamforming, 3D beamforming has distinct characteristics in beam pattern thus different effect on massive MIMO small cell. While 2D beamforming employs linear array antenna (LA), 3D beamforming is implemented based on planar flat/volume array antennas. Array elements of LA is aligned in a straight line separated from each other by equal or arbitrary length of distance measured in wavelength of carrier frequency. Due to the architectural limitation, LA can only form 2D beam pattern in either horizontal or vertical plane, thus it can only distinguish or separate users in different angles of either azimuth or elevation domain, lacking capability of identification in both domains at the same time. Therefore, 2D beamforming can not make full use of spatial resources. Contrary to 2D beamforming, 3D beamforming boasts capability of identifying users in full spatial dimension by forming 3D beam patterns in arbitrary cubic angle of directions, improving usage efficiency of spatial resources. This is very important for combating the increasing scarce of resources in wireless communications.

With the evolution trend of smaller, denser and smarter in cell, 3D beamforming technique emerges in massive MIMO wireless communications owing to the beneficial capability of controlling the strength of radiation field energy in different directions in spatial domain. An inherent property of 3D beamforming technique is the capability of emerging itself into existing wireless communication infrastructures and techniques seamlessly, further increasing system performances of data rate, throughput and capacity, without changing much of existing system physical architecture. Another beneficial characteristics of 3D beamforming lies in its capability of mitigating the deleterious effects of multipath, reducing both co-channel interference and multipath fading in the received signal simultaneously, thus achieving higher data rates [10]. Ref. [11] investigated beamforming performance in relay-assisted wireless communications. Ref. [12] analyzed performance of an optimal single stream beamforming scheme for a MIMO relay network with dual-hop fixed-gain amplify-and-forward (AF) relaying. Ref. [13] studied multi-cell cooperation based on coordinated multiple point joint processing and transmission (CoMP-JPT) with orthogonal beamforming. Ref. [14] proposed a beamforming scheme for massive MIMO transmission systems to achieve most of the gain inherent to a large array antenna without too much complexity. In millimeter wave (mm-Wave) beamforming, Ref. [15] presented recent results from channel measurement campaigns and the development of advanced algorithms and a prototype to verify the application possibility of mm-wave band may have for future cellular systems. Ref. [16] proposed a beamforming protocol that is realized in media access control (MAC) layer on top of multiple physical layer (PHY) designs. Ref. [17] proposed a beam searching algorithm and a codebook design for multilevel beamforming in outdoor mm-wave communication systems. Ref. [18] discussed beamforming application for large array antennas in mm-wave systems, proposed diversity eigen-beamforming methods. Challenges emerge in 3D beamforming when the number of array antenna elements approaches to very large or massive. There has been continuous increasing demand for high efficient 3D beamforming scheme and algorithms.

Performances of 3D beamforming wireless communications obviously rely on the properties of beam

pattern. Therefore, it is of importance to investigate in depth the properties and applications of 3D beamforming, laying sound ground for analyzing system performance of wireless massive MIMO small cell communication. However, most researches in beamforming have been focused on system-level or higher-layer performance analysis in terms of capacity and throughput, only a few studies performed analysis from the viewpoint of physical level.

In this paper, we analyze 3D beamforming property and applications in wireless communications based on physical structure of array antenna, addressing on the 3D beampattern property of plane rectangular array antenna beamforming. The contributions of this paper include the following. Firstly, we formulate array vector based on rectangular array antenna, and derive formulas pertaining to antenna beampattern parameters in detail. Secondly, we analyze the effect of array antenna configuration and the small cell radius on 3D beamforming. Thirdly, we apply 3D beamforming to small cell wireless communication scenario by analyzing single cell capacity gain over 2D beamforming in terms of number of users.

The rest of the paper is organized as follows: Section 2 introduces 3D beamforming system and signal models and formulate 3D beam pattern. Section 3 analyzes characteristics of 3D beampattern for understanding principle of 3D beamforming from the viewpoint of physics aspect. Section 4 applies 3D beamforming to small cell wireless system and shows numerical results. Section 5 concludes the paper.

## 2 System model

Figure 1 shows a 3D beamforming massive MIMO small cell system. Based on Rayleigh channel model, We analyze 3D beamforming characteristics of a planar rectangular array antenna in terms of parameters of beampattern and system capacity. Figure 2 shows a 3D beamforming scenario using a planar rectangular array and Figure 3 is the coordinates used in this paper. Without loss of generality, assume a planar rectangular array comprising a set of  $M \times N$  isotropic array elements in  $x - y$  plane with equally interelement spacing,  $d_x, d_y$ , in both  $x$  and  $y$  axes perpendicular to horizontal plane [10, 19].  $M, N$  denote the number of antenna elements in  $x$  and  $y$  coordinates, respectively. To be in accordance with terms and definitions commonly used in beamforming techniques, we define the direction of angle between User  $i$  ( $U_i$ ) and coordinate axis  $z$  as an elevation or vertical angle and denote it by  $\theta$ , and  $\phi$  denote a user's direction of angle (DOA) in horizontal plane, or  $x$ - $y$  coordinate plane. Let  $w, \lambda$  be angular frequency and wavelength of carrier signal, respectively. In addition, the initial phase of impinging signals on ( $m$ th,  $n$ th) element leads that in the ( $(m - 1)$ th,  $(n - 1)$ th) element by phase shifts of  $(\beta_x, \beta_y)$  radians projected to axes  $x, y$ , respectively. Thus, it is obvious that  $(\beta_x, \beta_y)$  is zero on  $z$  axis. In other scenarios,  $(\beta_x, \beta_y)$  will be determined based on user's location, keeping one-to-one mapping with DOA of users,  $w_{mn}$  denotes the weight of ( $m$ th,  $n$ th) element of an array antenna.

In this section, we introduce antenna manifold of a rectangular planar array, assuming a reference phase to be zero. We then formulate beampattern function for analysis of system performance. A planar rectangular array antenna can be viewed as an  $M$  linear array of  $N$  elements, or vice versa, as an  $N$  linear array of  $M$  elements [20].

Refer to Figure 3, the manifold vector of the array antenna in  $x, y$  coordinates is denoted by  $\mathbf{F}_x, \mathbf{F}_y$ , respectively.

$$\mathbf{F}_x = \left[ a_0, a_1 e^{j(\psi_1 + \beta_x)}, \dots, a_m e^{jm(\psi_1 + \beta_x)}, \dots, a_{M-1} e^{j(M-1)(\psi_1 + \beta_x)} \right], \quad (1)$$

$$\mathbf{F}_y = \left[ b_0, b_1 e^{j(\psi_2 + \beta_y)}, \dots, b_n e^{jn(\psi_2 + \beta_y)}, \dots, b_{N-1} e^{j(N-1)(\psi_2 + \beta_y)} \right], \quad (2)$$

where  $a_m, b_n$  is the weight of the  $m$ th,  $n$ th element of the array antenna, respectively, and  $m = 0, 1, \dots, M - 1; n = 0, 1, \dots, N - 1; \psi_1 = kd_x \sin \theta \cos \phi, \psi_2 = kd_y \sin \theta \sin \phi; k = 2\pi/\lambda; \beta_x = -kd_x \sin \theta_0 \cos \phi_0, \beta_y = -kd_y \sin \theta_0 \sin \phi_0; d_x, d_y$  is interelement spacing;  $\theta_0, \phi_0$  is DOA of intended user or users.  $\beta_x, \beta_y$  is the function of user DOA determined by the location of users in small cell wireless communication system.

We obtain the manifold matrix  $\mathbf{F}_{xy}$  of an  $M \times N$  elements rectangular array antenna according to multiplication principle of beamforming. Thus,  $\mathbf{F}_{xy}$  is the product of subarray manifold vectors  $\mathbf{F}_x$  and

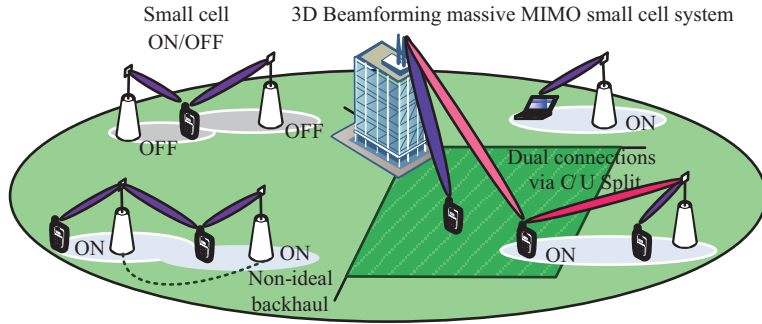


Figure 1 (Color online) 3D beamforming massive MIMO small cell system.

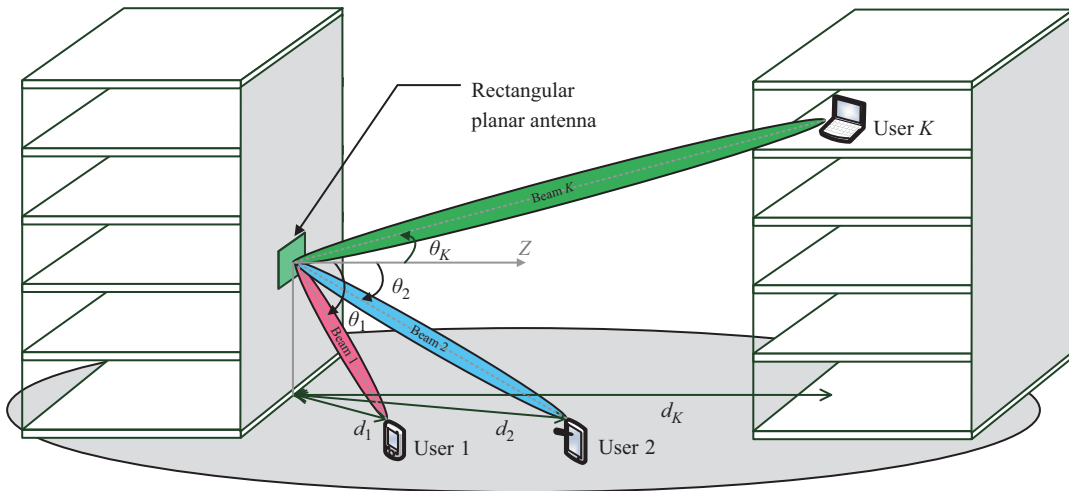


Figure 2 (Color online) 3D beamforming system model  $d_1, d_2, d_k$ : Distance between user and small cell.

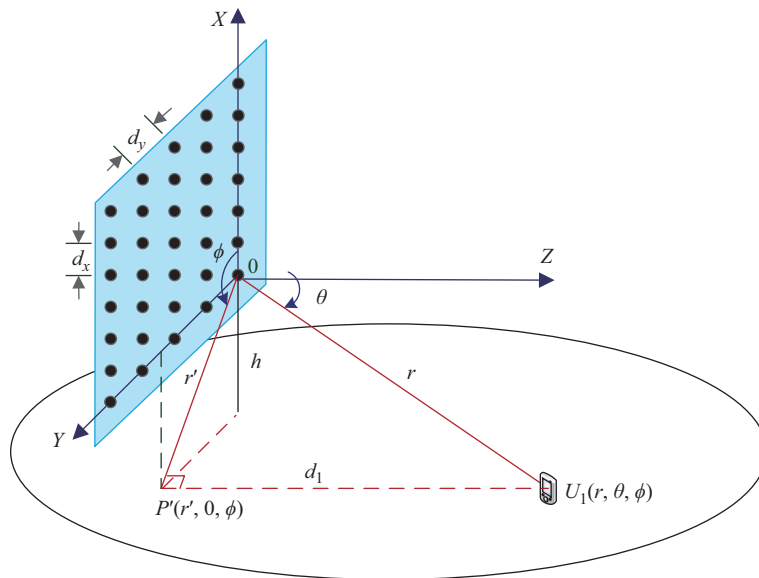


Figure 3 (Color online) Coordinates of 3D beamforming rectangular array antenna.

$\mathbf{F}_y$ . In essence, we can take either one of  $\mathbf{F}_x$  and  $\mathbf{F}_y$  manifold vectors as an array antenna manifold vector, formulating an array factor (AF) by summing up all the elements in the vector, and take the other one as radiation factor of an equivalent antenna ‘element’.

$$\mathbf{F}_{xy} = \mathbf{F}_x^T \times \mathbf{F}_y. \quad (3)$$

Therefore, we have obtained manifold of the rectangular planar array antennas containing  $M \times N$  weights. Furthermore, We introduce an AF and find out beampattern function based on the AF:

$$\text{AF} = \sum_{m=0}^{M-1} \sum_{n=0}^{N-1} w_{mn} e^{j[m(\psi_1 + \beta_x) + n(\psi_2 + \beta_y)]}, \quad (4)$$

where  $w_{mn} = a_m \times b_n$  is the weight of ( $m$ th,  $n$ th) element of an array antenna. Assuming unified amplitude signals,  $|a_m| = |b_n| = 1$ ,  $|w_{mn}| = 1$ . Thus, the characteristics of the rectangular array antenna are completely determined by the phase relationship among the elements and the phase difference is proportional to the interelement spacing measured in wavelength  $\lambda$ . Notice that this assumption does not result in loss of generality because of the fact of beampattern multiplication principle. Also notice that the manifold function of a rectangular planar array antenna is a Vandermonde vector. Thus, we can obtain 3D beampattern function based on AF.

Beampattern is referred to the envelope of radiation of electromagnetic wavefront in spatial domain. It is either a function or a plot describing the properties of an antenna directionality. The pattern can be a function describing the electric or magnetic fields. In that case, the pattern is a field pattern. Beampattern can also be the radiation intensity of power in terms of spatial angle. In theoretical analysis, field beampattern is more convenient to use than power, because it can be obtained directly from the multiplication of radiation manifold of elements in an array antenna and array antenna manifold, or from the multiplication of element radiation factor and array factor. We take field strength pattern as the measure of beampattern for analysis. In this case, a beampattern function is equal to the amplitude of AF and we may rearrange this function in the following form:

$$\text{BP} = |\text{AF}| = \frac{\sin(\frac{M}{2}\psi_x)\sin(\frac{N}{2}\psi_y)}{M N \sin(\frac{\psi_x}{2})\sin(\frac{\psi_y}{2})}, \quad (5)$$

where BP denotes beampattern function,  $\psi_x = \frac{2\pi}{\lambda} d_x \sin\theta \cos\phi + \beta_x$ ,  $\psi_y = \frac{2\pi}{\lambda} d_y \sin\theta \sin\phi + \beta_y$ . In the next section, we analyze 3D beampattern characteristics in massive MIMO small cell scenario and investigate the relationships among array configurations, beampattern parameters and system performance such as capacities. The analysis can be of usefulness in system design.

### 3 Analysis of 3D beamforming characteristics

We analyze characteristics of 3D beamforming in massive MIMO small cell, discussing the relationship between parameters of maximum beamforming gain  $G_A$ , half power beamwidth (HPBW) and direction of angle  $(\theta_0, \phi_0)$  of user steered, RF angular frequency  $w$  and interelement spacing  $d_x, d_y$  in terms of RF signal wavelength  $\lambda$ . Specifically, we investigate 3D beampattern nulls, maximum gain and beamwidth of mainlobe. Those parameters are among main factors affecting the performance of 3D beamforming.

Eq. (5) can be decomposed to two separable factors,  $|\text{AF}_{mx}| = \frac{\sin(\frac{M}{2}\psi_x)}{M \sin(\frac{\psi_x}{2})}$ ,  $|\text{AF}_{ny}| = \frac{\sin(\frac{N}{2}\psi_y)}{N \sin(\frac{\psi_y}{2})}$ . Without loss of generality, we analyze 3D beamforming characteristics based on the factors for analytical simplicity.

(1) 3D Beampattern Nulls. We analyze Eq. (5) to find 3D beampattern nulls of interest. The first pair of nulls is outside the mainlobe and it determines the minimum interference-free beamwidth as well as highest capability of resolution of the antenna. Notice that different beamforming properties exist between macrocell and small cell scenarios in both 2D and 3D. Second pair of nulls determines the property of the largest sidelobe. In general, the maximum interference to adjacent users occurs here.

In essence, the first null determines the maximum beamwidth of an array antenna, representing the maximum angular resolution ability of the antenna. In wireless communications scenario, this is the minimum angle between two users that can be distinguished and without interference to each other. We investigate the relationship between the angle of nulls and the number of array antenna element, or equivalently, between angular resolution capability and physical aperture of array antenna. Based on this,

we could determine the maximum distribution density of users in a given area, and further analyze system performance, such as throughput, capacity. In system design scenario, we can determine the number of array antenna element given the distribution density of users. In addition, physical angle resolution can be improved by employing proper signal processing techniques, so that realizing super-resolution. As can be seen, the null is an important parameter in beamforming.

Observing Eq. (5), we can find nulls by zeroing either factors of its numerator,

$$\sin\left(\frac{M\psi_x}{2}\right)\sin\left(\frac{N\psi_y}{2}\right) = 0, \quad (6)$$

which can be translated to either  $\frac{1}{2}M\psi_x = k\pi$  or  $\frac{1}{2}N\psi_y = l\pi$ , where  $k, l = 0, \pm 1, \pm 2, \dots$ . It is obvious that beampattern nulls depend on multiple parameters: the number of array antenna element  $MN$ , vertical angle  $\theta$ , horizontal angle  $\phi$ , array antenna interelement distance  $(\frac{d_x}{\lambda}, \frac{d_y}{\lambda})$ , and user's position or angles of direction  $(\beta_x, \beta_y)$ .

We analyze the effect of parameters  $M, N$ , angles  $\theta, \phi$  and  $\beta_x, \beta_y$  on the 3D beamforming characteristics, and then analyze system capacity in terms of number of users within a small cell coverage, radius  $R$ , without interference with each other, finding the capacity gain of 3D beamforming over 2D scenario. we have

$$\theta_{\text{null}} = \sin^{-1}\left(\frac{\lambda}{2\pi d_x}\left(\pm\frac{2\pi m}{M} - \beta_x\right)\right), \quad m = 1, 2, \dots \quad (7)$$

and

$$\phi_{\text{null}} = \sin^{-1}\left(\frac{\lambda}{2\pi d_y}\left(\pm\frac{2\pi n}{N} - \beta_y\right)\right), \quad n = 1, 2, \dots \quad (8)$$

subject to  $\{|\frac{\lambda}{2\pi d_x}(\pm\frac{2\pi m}{M} - \beta_x)| \leq 1\} \cup \{|\frac{\lambda}{2\pi d_y}(\pm\frac{2\pi n}{N} - \beta_y)| \leq 1\}$ .

(2) Maximum array gain. We could find array antenna's maximum Gains in the mainlobe based on (5). Furthermore, we can analyze variation of the maximum gain with parameters of DOA and the number of array antenna element. Maximum gain describes the performance of an array antenna's capacity of transmitting power or receiving signals in the intended DOA. This maximum gain is interference to other users.

The maximum gain of array antenna will be obtained as the denominator of (5) approaches zero,

$$\left|MN\sin\left(\frac{\psi_x}{2}\right)\sin\left(\frac{\psi_y}{2}\right)\right| = 0. \quad (9)$$

(3) Mainlobe beamwidth. Half power beamwidth (HPBW) is the angle between 3 dB points of a radiation pattern [10], varying with parameters such as number of array antenna element, direction of arrival angles, interelement distance in terms of wavelength and frequency. Similar to the angle of first Null, HPBW also describes the beamwidth of a beampattern, but it describes mainlobe beamwidth within half-power points. In 3D beampattern scenario, HPBW is measured by the term of beam solid angle in steradians. A beam solid angle is a volume angle in which antenna power being radiated, and unit steradians is the beam solid angle formed by the surface area  $r^2$  of a sphere. In planar rectangular array antenna, the beam solid angle can be decomposed into azimuth and elevation angles. We may find 3D beampattern solid angle HPBW based on Eq. (5).

In essence, Eq. (5) is a formula of unity gain. Therefore, the mainlobe HPBW can be obtained by having it equal to  $\frac{1}{\sqrt{2}}$ .

$$\left|\frac{\sin(\frac{M}{2}\psi_x)\sin(\frac{N}{2}\psi_y)}{MN\sin(\frac{\psi_x}{2})\sin(\frac{\psi_y}{2})}\right| = \frac{1}{\sqrt{2}}. \quad (10)$$

In addition, the influence to the variation of beampattern characteristics caused by parameters of array antenna will be different in macrocell and small cell due to multiple factors, such as, user probability distribution function in term of the parameter set.

**Table 1** Mainlobe and second nulls of beampattern

$\theta_{\text{null}}$	$\phi_{\text{null}}$	$M$	$N$
14.48°	30°	8	8
7.18°	14.48°	16	16

**Table 2** Beampattern nulls in broadside

$\theta_{\text{HPBW}}$	$\phi_{\text{HPBW}}$	$M$	$N$
12.71°	12.71°	8	8
6.35°	6.35°	16	16

## 4 Numerical results

In order to obtain optimal performance for 3D beamforming in small cell scenario, the number of array antenna elements should be sufficiently large [21], for small cell demands much narrower beamwidth than macrocell and other traditional application scenarios in comparatively much shorter distance in order to distinguish users in small cell and thus increase system capacity. However, dramatically increased number of elements leads to high computing capability which further arising the challenge of demanding new 3D beamforming methods and algorithms that are highly efficient with acceptable performance. In reality, the number of array antenna elements is finite and it should not be too large. Therefore, tradeoffs have to be considered between performance and efficiency. Thus, a natural question is: how large of an array antenna is sufficient for a given performance? [22]. What is the relationship between system performance and parameters of an array antenna, such as the number of array antenna elements, carrier frequency?

In this section, we will investigate 3D beamforming characteristics in small cell from numerical perspectives, examining 3D beamforming based on (8)–(10), pertaining to beampattern nulls, beampattern maximum gain and beamwidth (HPBW) of a 3D beamforming, respectively.

Assume  $N = M = 8, 16$ , interelement spacing  $d_x = d_y = \frac{\lambda}{2}$ , carrier frequency  $f = 5, 30$  GHz, BS antenna height  $h = 30, 90$  m, that amount to the buildings of ten and thirty layers, BS coverage radius  $R = 30, 90, 900$  m, user one ( $U_1$ ) equipment (UE) antenna height  $h_u = 0$ .

(1) Beampattern nulls. We analyze mainlobe null based on (8) in vertical plane first and then extend to 3D beamforming case based on multiplication principle, as shown in Table 1.

The 1st and 2nd nulls is  $\theta_{\text{null}} = 14.48^\circ, 30^\circ$  for  $M = 8$ , and  $\theta_{\text{null}} = 7.18^\circ, 14.48^\circ$  for  $M = 16$ . Notice that the first null is approximately reciprocally proportional to the number of array antenna elements in the broadside of the antenna.

If  $\theta_0 = 70^\circ, \phi_0 = 0$ , corresponding to a large steering angle of user,  $\sin(70^\circ) = 0.9397$ , no null would exist within effective range in this case. Figure 4 shows 3D beamforming single-beam in different number of array antenna elements. Furthermore, Figure 5 illustrates 3D beamforming multiple-beam in multiple user scenario, respectively. As shown in Figures 4 and 5, the larger number of antenna elements, the smaller beamwidth of 3D beamforming beams and therefore, the higher resolution in beamspace.

(2) Maximum gain. Based on (9), it is obvious that the maximum gain of the antenna is the maximal gain of mainlobe and it occurs in the steering angle. Notice that this gain is unified in this paper, i.e., if  $\beta_x = 0^\circ, 30^\circ, 70^\circ$ , then the maximum gain is obtained in exactly those direction of angles and is unity.

(3) HPBW. This is a useful parameter in small cell performance analysis, because it determines system capacity of wireless communications corresponding to spacial resource efficiency. Figure 6 demonstrates the variations of 3D beamforming beamwidth in vertical plane with different number of array antenna elements and user locations. While the beamwidth will become wider at larger angle of user location, the variation is almost negligible compared with the beamwidth itself. However, the number of array antenna elements affects the beamwidth obviously. We analyze HPBW of 3D beamforming in vertical plane based on (10) and the number of beams within BS coverage area (in radius). In essence, this number amounts to capacity gain of 3D over 2D beamforming. Based on (10), we can find HPBW.

In broadside, the results are shown in Table 2. Further more, in  $\beta_x = \beta_y = 45^\circ$ , results are summarized in Table 3.

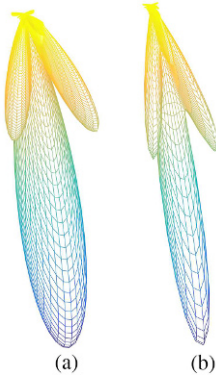


**Figure 4** (Color online) 3D beamforming, single beam. (a)  $N, M = 8$ ; (b)  $N, M = 16$ .

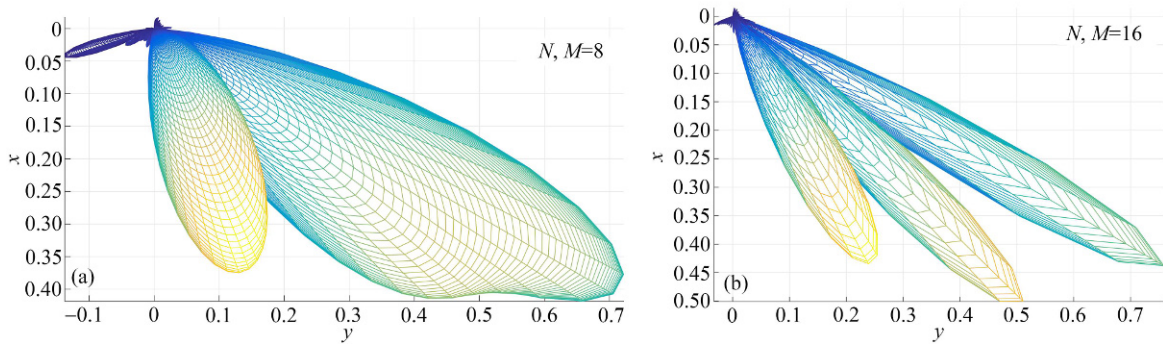


**Figure 5** (Color online) 3D beamforming, multiple users. (a)  $N, M = 8$ ; (b)  $N, M = 16$ .

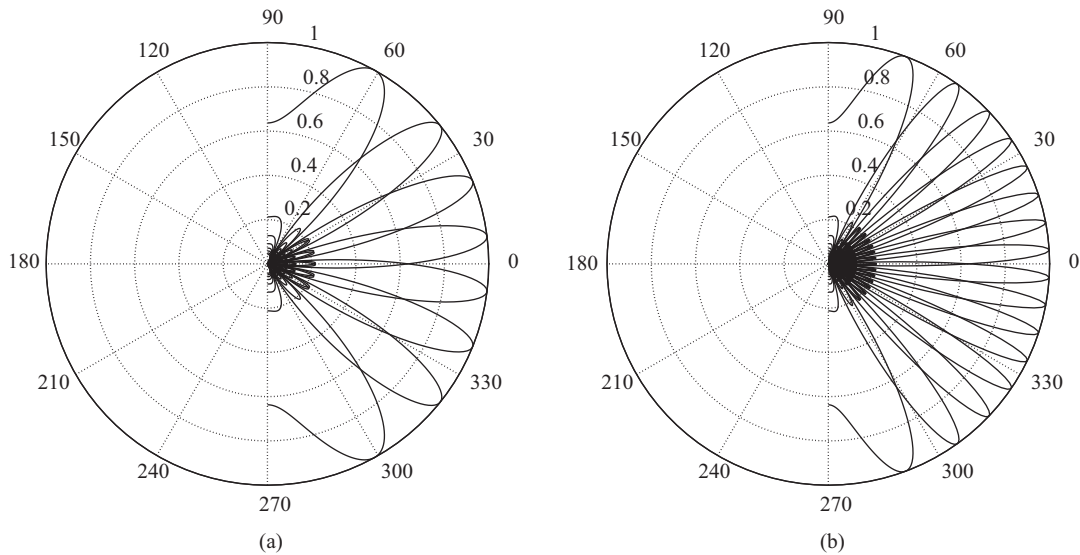


**Figure 6** Variations of 3D beamforming beamwidth in vertical plane. (a)  $N, M = 8$ ; (b)  $N, M = 16$ .

**Table 3** Beampattern nulls along diagonal direction

$\theta_{\text{HPBW}}$	$\phi_{\text{HPBW}}$	$M$	$N$
$13.05^\circ$	$13.05^\circ$	8	8
$6.51^\circ$	$6.51^\circ$	16	16

Notice that HPBW is reciprocally proportional to the number of array antenna elements. Thus, the HPBW will decrease by increasing the number of array antenna elements, thus improving 3D beamforming

**Table 4** Beampattern nulls with  $h = R$

$\beta_x$	$\beta_y$	$\theta$	$\phi$	$M$	$N$	$l$
0	0	12.71°	12.71°	8	8	3.54
0	0	6.35°	6.35°	16	16	7.08
45°	45°	12.71°	12.71°	8	8	3.45
45°	45°	6.35°	6.35°	16	16	6.91

**Table 5** Beampattern nulls with  $h \neq R$

$\beta_x$	$\beta_y$	$M$	$N$	$h$	$R$	$l$
0	0	8	8	30	90	5.63
0	0	16	16	30	90	11.26
45°	45°	8	8	30	90	5.48
45°	45°	16	16	30	90	10.99
0	0	8	8	30	900	6.93
0	0	16	16	30	900	13.86
45°	45°	8	8	30	900	6.75
45°	45°	16	16	30	900	13.53

performance.

Comparing the results in the scenarios of different values of  $\theta_0$ , we notice that the HPBW will tend to larger with the increase of elevating angle  $\theta_0$ .

Based on the HPBW and geometry structure of wireless communication systems, we could apply 3D beamforming to small cell communication with respect to capacity improvement. Assuming a single cell system with omnidirectional array antenna elements in small cell, we analyze the maximum number of orthogonal beams (different HPBW) in the RF coverage area denoted by  $l$ .

With  $h = R$ , numerical result is shown in Table 4. With  $h \neq R$ , we obtain the results shown in Table 5, where  $h$  stands for the height of array antenna in small cell station and  $R$  is the radius of RF coverage.

Observing Tables 4 and 5, we reach the following conclusion points.

- User's positions (steering angles  $\beta_x$ ) affect the maximum number of 3D beams, that is equivalent to the number of users without interference to each other.
- Within a given service area, contrasting to large radius  $R$  BS architecture, small radius system (small cell) will allow more number of BS, that is equivalent to more non-interference beams.
- Increasing the number of array antenna element will effectively improve array antenna resolution and thus increase the number of users in a given area of wireless communications.

## 5 Conclusion

We analyzed properties and performance of 3D beamforming deployed in wireless communications scenario from physics point of view. As shown in the analysis, 3D beamforming can greatly leverage 3D spacial resource efficiency, thus increase system capacity in wireless communications, laying solid foundations for improving throughput and capacity in small cell massive MIMO system.

## References

- 1 Zhu H, Wang J. Chunk-based resource allocation in ofdma systems — part i: chunk allocation. *IEEE Trans Commun*, 2009, 57: 2734–2744
- 2 Zhu H, Wang J. Chunk-based resource allocation in ofdma systems — part ii: joint chunk, power and bit allocation. *IEEE Trans Commun*, 2012, 60: 499–509
- 3 Zhu H. Radio resource allocation for ofdma systems in high speed environments. *IEEE J Sel Areas Commun*, 2012, 30: 748–759
- 4 Zhu H. Performance comparison between distributed antenna and microcellular systems. *IEEE J Sel Areas Commun*, 2011, 29: 1151–1163

- 5 Wang J, Zhu H, Gomes N. Distributed antenna systems for mobile communications in high speed trains. *IEEE J Sel Areas Commun*, 2012, 30: 675–683
- 6 Koppenborg J, Halbauer H, Saur S, et al. 3D beamforming trials with an active antenna array. In: *Proceedings of International ITG Workshop on Smart Antennas (WSA)*, Dresden, 2012. 110–114
- 7 Xia M, Wu Y-C, Aissa S. Non-orthogonal opportunistic beamforming: performance analysis and implementation. *IEEE Trans Wirel Commun*, 2012, 11: 1424–1433
- 8 Matthaiou M, de Kerret P, Karagiannidis G, et al. Mutual information statistics and beamforming performance analysis of optimized los mimo systems. *IEEE Trans Commun*, 2010, 58: 3316–3329
- 9 Wang J, Zhu H, Dai L, et al. Low-complexity beam allocation for switched-beam based multiuser massive mimo systems. *IEEE Trans Wirel Commun*, 2016, 15: 8236–8248
- 10 Gross F B. *Smart Antennas for Wireless Communications with Matlab*. New Yor: McGraw-Hill Companies, Inc., 2005
- 11 Rashid U, Tuan H, Kha H, et al. Joint optimization of source precoding and relay beamforming in wireless mimo relay networks. *IEEE Trans Commun*, 2014, 62: 488–499
- 12 Jayasinghe P, Jayasinghe L, Juntti M, et al. Performance analysis of optimal beamforming in fixed-gain AF MIMO relaying over asymmetric fading channels. *IEEE Trans Commun*, 2014, 62: 1201–1217
- 13 Lee H, Kim S, Lee S. Combinatorial orthogonal beamforming for joint processing and transmission. *IEEE Trans Commun*, 2014, 62: 625–637
- 14 Lee G, Park J, Sung Y, et al. A new approach to beamformer design for massive mimo systems based on k-regularity. In: *Proceedings of IEEE Globecom Workshops (GC Wkshps)*, Anaheim, 2012. 686–690
- 15 Roh W, Seol J-Y, Park J, et al. Millimeter-wave beamforming as an enabling technology for 5G cellular communications: theoretical feasibility and prototype results. *IEEE Commun Mag*, 2014, 52: 106–113
- 16 Wang J, Lan Z, woo Pyo C, et al. Beam codebook based beamforming protocol for multi-gbps millimeter-wave wpan systems. *IEEE J Sel Areas Commun*, 2009, 27: 1390–1399
- 17 Hur S, Kim T, Love D, et al. Millimeter wave beamforming for wireless backhaul and access in small cell networks. *IEEE Trans Commun*, 2013, 61: 4391–4403
- 18 Choi J. On coding and beamforming for large antenna arrays in mmwave systems. *IEEE Wirel Commun Lett*, 2014, 3: 193–196
- 19 Trees H V L. *Optimum Array Processing*. Hoboken: John Wiley and Sons, Inc, 2002
- 20 Hitachi America Lab. Full-dimensional mimo for future cellular networks. In: *Proceedings of Wireless Systems Research Laboratory (WSRL)*, Michigan, 2014
- 21 Narasimhan T, Raviteja P, Chockalingam A. Large-scale multiuser sm-mimo versus massive mimo. In: *Proceedings of Information Theory and Applications Workshop (ITA)*, San Diego, 2014. 1–9
- 22 Huh H, Caire G, Papadopoulos H, et al. Achieving “massive mimo” spectral efficiency with a not-so-large number of antennas. *IEEE Trans Wirel Commun*, 2012, 11: 3226–3239